Journal of Computational Acoustics, Vol. 9, No. 3 (2001) 1215–1225

AIRBORNE ACOUSTICS OF EXPLOSIVE VOLCANIC ERUPTIONS*

MICHAEL J. BUCKINGHAM

Marine Physical Laboratory, Scripps Institution of Oceanography, University of California, San Diego, 9500 Gilman Drive, La Jolla, CA 92093-0213, USA

Also affiliated to: Institute of Sound and Vibration Research, The University, Southampton SO17 1BJ, England

MILTON A. GARCÉS

University of Hawaii, Manoa, P.O. Box 1599, Kailua-Kona, HI 96745-1599, USA

Received 6 October 1999
Revised 16 April 2000

A recently developed theoretical model of the airborne acoustic field from an explosive volcanic eruption of the Strombolian type is described in this article. The magma column is assumed to be a circular cylinder, which is open to the atmosphere at the top, and which opens into a large magma chamber below. The magma itself is treated as a fluid, and the surrounding bedrock is taken to be rigid. An explosive source near the base of the magma column excites the natural resonances of the conduit. These resonances result in displacement of the magma surface, which acts as a piston radiating sound into the atmosphere. The source is modeled in much the same way as an underwater explosion from a high-explosive chemical such as TNT, although in the case of the volcano the detonation mechanism is the ex-solution of magmatic gases under extremely high hydrostatic pressure. The new theory shows compelling agreement with airborne acoustic signatures that were recorded in July 1994 at a distance of 150 m from the western vent of Stromboli volcano, Italy. The theoretical and observed power spectra both display the following features: (1) four energetic peaks below 20 Hz, identified as the first four longitudinal resonances of the magma column; (2) a broad minimum around 30 Hz, interpreted as a source-depth effect, occurring because the source lay close to nulls in the fifth and sixth longitudinal resonances and thus failed to excite these modes; and (3) radial resonance peaks between 35 and 65 Hz. On the basis of the theory, an inversion of the acoustic data from Stromboli yields estimates of the depth ($\approx$ 100 m) and radius ($\approx$ 16 m) of the magma column as well as the depth ($\approx$ 83 m), spectral shape and peak shock-wave pressure ($\approx$ 1 GPa) of the explosive source. Most of the parameters estimated from the acoustic inversion compare favorably with the known geometry and source characteristics of Stromboli.

1. Introduction

Ground-propagating seismic signals from volcanic activity are commonly used to determine both the internal structure of a volcano and the characteristics of the source. By comparison,

*Presented at ICTCA'99, the 4th International Conference on Theoretical and Computational Acoustics, May 1999, Trieste, Italy.

little attention has been paid to the airborne sound generated by an erupting volcano. Yet, potentially, the airborne acoustic signature contains important information about the dimensions of the conduit, the material and chemical properties of the magma, the depth of the source, and even the nature of the source mechanism.

Moreover, the atmosphere is essentially homogeneous over practical measurement ranges, and hence introduces little distortion into airborne acoustic signals. In contrast, seismic signals traveling through the bedrock between the volcanic source and a seismometer located on the flank of the mountain are heavily modified by the highly irregular, and largely unknown, properties of the sub-surface propagation path. It would seem, then, that airborne acoustic signatures offer some advantage as the basis of an inversion procedure for recovering information on the internal structure of the volcano.

The first systematic recordings of airborne sounds from erupting volcanoes were made by Perret.[1] More recently airborne acoustic signatures have been reported by several other investigators.[2–7] The sounds are produced by a variety of mechanisms, including high-pressure gas jets issuing from the surface of the magma, mild explosions occurring at the top of the magma column,[8] and highly energetic explosions deeper in the conduit associated with the ex-solution of magmatic gases.[9]

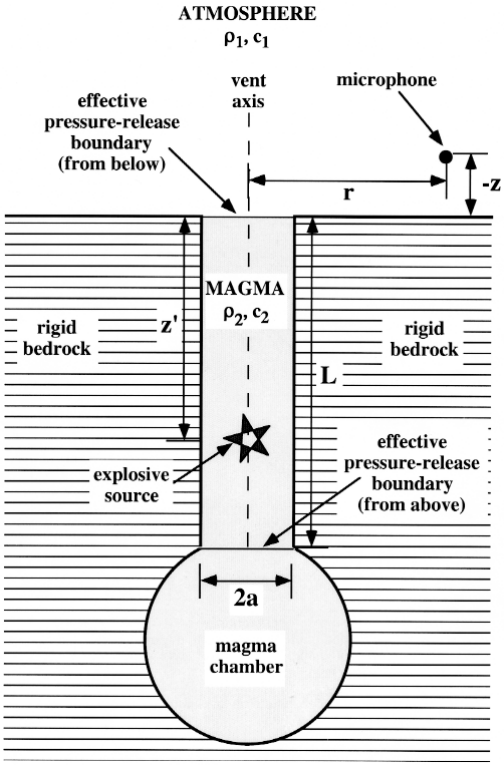

Fig. 1. Axi-symmetric (2-D) model of the magma column and atmosphere used in the analysis. Density, ρ, and sound speed, c, are taken to be constant in the atmosphere and magma, denoted by subscripts 1 and 2, respectively.

Explosive eruptions of the Strombolian type, which occur one hundred or so meters beneath the surface of the magma, are the topic of this article. A recently developed analytical model[10] of the airborne sound field generated by an energetic source near the base of the magma column is reviewed and summarized here. In the analysis, the magma column is represented as a right circular cylinder in which a point source is located on axis (Fig. 1), creating an azimuthally uniform sound field. Thus, in the model, the field depends on just two spatial variables, horizontal range from the axis and elevation above or below ground level.

When the source detonates, longitudinal and radial resonances are excited in the magma column, and the magma surface, which is treated as a pressure-release boundary, is displaced from its equilibrium position. The vertical displacements over the surface of the magma are not uniform but are characterized by the normal-mode structure of the acoustic field in the magma column. In effect, the motion of the magma surface acts as a complicated piston, coupling the sound field in the magma column into the atmosphere. Through this coupling, the airborne sound field retains the resonant character of the field in the magma column: each mode in the magma column excites a corresponding atmospheric sound field with its own characteristic spatial and spectral structure. The total field at any point in the atmosphere is the sum of the contributions excited by all the modes in the magma column. Thus, the model yields a complete analytical description of both the pulse shape and power spectrum of the airborne acoustic signature. These solutions, in the time and frequency domains, are both in the form of a sum of normal modes.

2. Green's Function Analysis

To obtain the time and frequency domain solutions, two wave equations are set up, one (inhomogeneous) for the acoustic field in the magma column and the other (homogeneous) for the field in the atmosphere:

$$\nabla^2 g_1 - \frac{1}{c_1^2}\frac{\partial^2 g_1}{\partial t^2} = 0\,, \quad \text{(atmosphere)} \tag{2.1}$$

and

$$\nabla^2 g_2 - \frac{1}{c_2^2}\frac{\partial^2 g_2}{\partial t^2} = -Q\delta(t)\delta(r - r')\,, \quad \text{(magma column)}\,. \tag{2.2}$$

In these expressions, t is time, c_i is the speed of sound (taken to be constant), Q is the source strength, $g_i(t)$ is the velocity potential [i.e., the particle velocity $u_i(t) = -\nabla g_i(t)$], and the vectors r' and r identify the source and receiver positions, respectively. The subscript $i = 1, 2$ indicates that a variable is associated with region 1, the atmosphere, or region 2, the magma column (Fig. 1). Initially, the on-axis-source term on the right of the inhomogeneous equation is taken to be a delta function in time and space, which yields the Green's function fields in the magma and the atmosphere. Once the Green's functions have been determined, the field generated by an explosive source is obtained by a standard multiplication in the frequency domain between the Green's function and the (complex) source spectrum.

A Neumann (acoustically rigid) boundary condition is assumed for the curved, vertical surface of the magma column, and also for the horizontal surface of the bedrock surrounding the vent. At its base, the magma column opens out into a vast magma chamber, which gives rise to a large impedance difference between the two domains. This impedance difference is approximately equivalent to a pressure-release boundary terminating the magma column (Fig. 1). At the surface of the magma, strictly there must be continuity of the normal component of particle velocity and continuity of pressure across the boundary. However, because the density ratio between the magma and the atmosphere is so large, in the region of 1000:1, the upper boundary of the magma effectively acts as a pressure release surface for radiation incident from below. This effective Dirichlet (pressure-release) boundary condition (Fig. 1) is important to recognize because it means that the fields in the magma and the atmosphere are separable and hence that the problem is tractable.

As it is a pressure-release boundary, the surface of the magma, in response to the acoustic field below, undergoes velocity perturbations in the vertical. This surface velocity field, which is determined from the general solution of the inhomogeneous wave equation for the field in the magma column, provides the coupling between the field in the magma and the field in the atmosphere. The field above the surface is found by solving the homogeneous wave equation for the field in the atmosphere, subject to the appropriate velocity distribution across the vent.

The two wave equations are solved by standard integral transform techniques. First, a Fourier transform with respect to time is performed, to produce reduced wave (i.e., Helmholtz) equations. For the field in the magma column, a finite Fourier sine transform over depth and a finite Hankel transform over horizontal range are applied to the inhomogeneous Helmholtz equation. Application of the corresponding inverse transforms yields the field in the magma column as an infinite sum of normal modes. From this solution, the coupling field over the surface of the magma may be determined.

The airborne sound field is then found by applying a Hankel transform in horizontal range to the homogeneous Helmholtz equation. The resultant ordinary differential equation is solved subject to the velocity boundary condition across the vent, and an inverse Hankel transform is applied to the result, to obtain an expression for the frequency-dependent field in the atmosphere. As with the solution for the field in the magma column, the expression for the sound field in the atmosphere is an infinite sum of normal modes. The modal coefficients take the form of a finite integral over the radius of the vent, a, which is evaluated using a combination of asymptotic techniques and numerical integration. A full account of the analysis may be found in Ref. 10.

3. High-Frequency Limit

In the limit of high frequency the analysis of the integral for the modal coefficients simplifies considerably. In essence, it is found that the eigenrays associated with each of the individual longitudinal modes in the magma column project into the atmosphere as a parallel-sided beam of sound, depicted by the arrows in Fig. 2. Actually, because of the axial symmetry

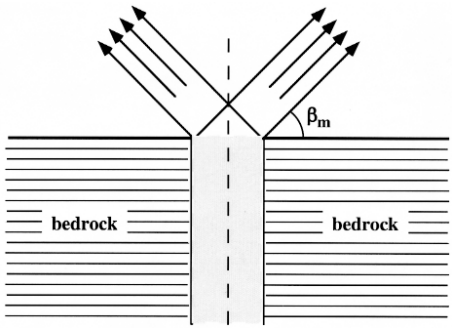

Fig. 2. High-frequency, parallel, parallel-sided beam of sound (arrows) associated with the mth mode radiating into the atmosphere.

of the problem, the beam is conical, a solid of revolution. The angle of elevation, β_m, of the beam corresponding to the mth mode is related to the grazing angle, α_m, of the associated eigenray in the magma column through Snell's law:

$$\frac{\cos\,\beta_m}{c_1} = \frac{\cos\,\alpha_m}{c_2} \tag{3.1}$$

where c_1 and c_2 are, respectively, the speed of sound in the atmosphere and in the magma. From an elementary argument based on upward and downward travelling plane waves in the magma column, the angle α_m is found to be given by the expression

$$\sin\alpha_m = \frac{m\pi c_2}{\omega L}\,, \tag{3.2}$$

where ω is angular frequency and L is the depth of the magma column (see Fig. 1).

The total field in the atmosphere is, of course, the superposition of the contributions from all the modes in the magma column. Figure 3 is a sketch of the high-frequency field distribution for the cases of a fast ($c_2 > c_1$) and slow ($c_2 < c_1$) magma. The latter condition

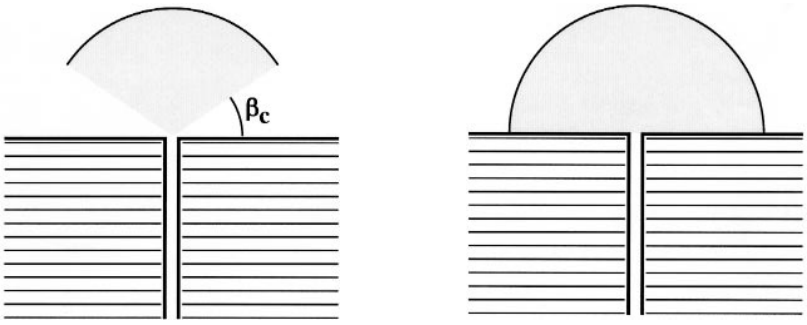

(a) (b)

Fig. 3. Sketch depicting the distribution (shading) of high-frequency sound in the atmosphere. (a) Fast magma: no acoustic energy propagates at elevation angles less than β_c; (b) Slow magma: acoustic energy is essentially uniformly distributed through all elevation angles between 0 and $\pi/2$.

could occur if the magma were highly vesiculated. The fast magma shows a critical angle, β_c, for radiation incident from above, the result of which is that all the sound exits the vent at elevation angles greater than β_s. Thus, in this case, no sound propagates horizontally. In contrast, the slow magma shows a critical angle for radiation incident from below, but this does not constrain the angular distribution of the sound energy in the atmosphere. In this case, the sound is more or less uniformly distributed through all elevation angles.

4. Diffraction

Although Eqs. (3.1) and (3.2) were derived from the full wave-theoretic analysis, they are in effect a result of geometrical (ray) acoustics. These two equations, and the sound field illustrated in Fig. 2, represent behavior that would be observed in the limit of high frequency. In this limit, a clear physical picture of the spatial structure of the airborne sound from the volcano emerges from the theory. However, the high-frequency, geometrical description has limited application in interpreting actual volcano sounds because the spectrum of the radiated, explosive acoustic signature is almost always rich in low frequencies. "Low" in this context implies wavelengths (in air) that are comparable with the aperture of the vent, a condition which obtains when the Helmholtz number of the vent, $\omega a/c_1$, is less than 2π.

In this low-frequency regime, diffraction from the edge of the vent is significant, the main effect of which is to broaden the airborne beams of sound. At sufficiently low frequencies, the broadening is so pronounced that the sound intensity in the atmosphere associated with a given longitudinal mode is essentially independent of elevation angle. Such behavior, of course, is not described by Eqs. (3.1) and (3.2). To take account of diffraction, it is necessary to return to the integral for the modal coefficients in the full wave solution for the airborne Green's function. The technique used to evaluate this integral is lengthy but fairly straightforward, as described by Buckingham and Garcés.[10] The resultant expressions for the integral, as well as being essentially exact, are fast to compute, allowing the mode sum to be evaluated efficiently on a desktop computer.

An important consequence of the beam broadening is that, even with a fast magma, low-frequency sound may propagate away from the vent at elevation angles below the critical grazing angle, β_c (unlike the high-frequency situation shown in Fig. 3(a). It follows that a microphone on the flank of the mountain will be ensonified by low frequencies regardless of whether the magma is fast or slow. Examples of the spatial distribution of airborne sound energy, computed for fast and slow magmas over a frequency range between 10 Hz and 200 Hz, can be found in Buckingham and Garcés.[10]

5. The Explosive Source

The airborne pressure waveform at any point in the atmosphere depends not only on the acoustic propagation conditions but also on the spectral shape of the explosive source. Although the details of the source mechanism are not fully understood, there is some evidence to suggest that an explosive eruption is the result of the sudden expansion of volcanic

gases which come out of solution as the pressure drops when the magma ascends through a constriction.[9,11–13]

Whatever the actual source mechanism, a reasonable, simple model of the detonation would seem to be a radially oscillating bubble of gas, much like that formed by an underwater explosion from a high-explosive chemical such as TNT.[14–17] The origin of the gas bubble is different in the two cases, but the effect is similar. The radial oscillations experienced by the bubble give rise to a sequence of pressure pulses, as illustrated in Fig. 4. Initially, the bubble expands very rapidly, creating a high pressure peak followed by a shock wave. As the expansion continues, the bubble passes through the radius at which it would be in equilibrium with the environment and finally reaches a maximum size, at which point the rate of growth is zero and the pressure is a minimum. The bubble then starts to collapse, again passing through the equilibrium radius, until a minimum size is reached where the pressure is a maximum. These oscillations, with reducing excursions about the equilibrium size, continue as the bubble comes into equilibrium with its environment (Fig. 4). Thus, the radiated pressure waveform consists of a shock wave followed by a succession of cusp-like bubble pulses.

The radially oscillating bubble acts as an acoustic monopole, which is an efficient source of sound. To model the radiated pressure pulse, a simple empirical pulse-shape function is adopted:

$$P_s(t) = P_o(1 - \alpha t) \exp -\beta t \,, \tag{5.1}$$

where $t \geq 0$. In fact this function, which has only one zero crossing, occurring at time $t = 1/\alpha$, provides a reasonable representation of the shock wave but neglects the subsequent bubble pulses. The bubble pulses could be represented by including higher-order terms in the polynomial preceding the exponential function in Eq. (5.1).

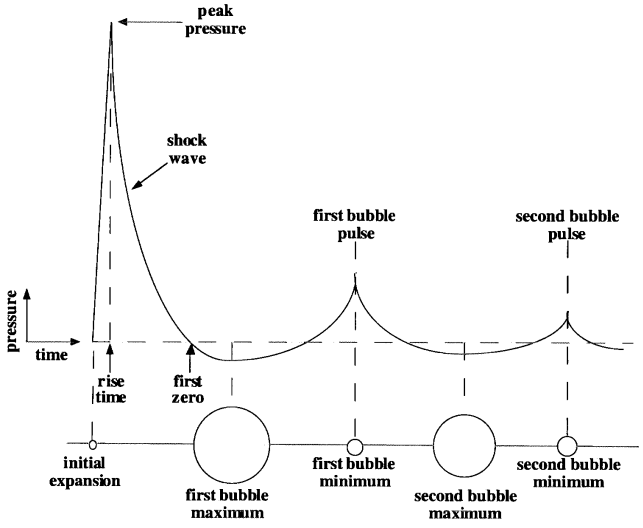

Fig. 4. Gas bubble oscillations in the magma column and the associated pressure waveform.

On Fourier transforming Eq. (5.1), the power spectrum of $P_s(t)$ is found to show a single maximum at $\omega = \omega_m = \omega$, rolling off on either side at -6 dB per octave. This simple spectral shape may be multiplied with the spectrum of the Green's function for the airborne sound, to obtain an estimate of the spectrum of the acoustic arrival at a microphone in the atmosphere.

6. Stromboli

In July 1994, we recorded many explosive sounds from the western vent of Stromboli volcano, Italy. The microphone was at a distance of 150 m from the vent, at a height above the mountainside of 1.5 m. A representative example of the average power spectrum of one of the Strombolian sounds is shown in Fig. 5. The Welch spectral estimation technique[18] was used to obtain this spectrum, with 12 time windows, 67% overlap, and a spectral resolution of 1.17 Hz. The finite frequency-cell width accounts for the fact that the level of the measured spectrum does not fall to zero as the frequency approaches zero, even though the associated pressure pulse has a zero mean.

Superimposed on the observed spectrum (dashed line) in Fig. 5 is a theoretical spectrum (solid line) derived from the full-wave theory described above. The parameters used in evaluating the theory were representative of Stromboli, whose basic geometry and geophysical properties have been investigated over recent years using a variety of techniques and are now moderately well established.[19] In particular, the depth of the magma column was set at 100 m, the depth of the explosive source was taken as 83.3 m, and the sound speed in the magma was assigned a value of 1000 m/s, which is consistent with a volume fraction of gas in the magma of approximately 2×10^{-5}. The peak pressure of the shock wave was taken to be 1 GPa.

The measured and theoretical spectra show a number of similar features, labeled A to G in Fig. 5. Of these features, A–D are the first four longitudinal modes of the magma column, occurring at multiples of 5 Hz. The trough or minimum labeled E is an effect of the source depth, which is close to nulls in longitudinal modes 5 and 6 and hence excites these resonances so weakly that they are essentially absent from the spectrum. Moving to slightly higher frequencies, the region between F and G contains two broad peaks, which are attributed to the first set of radial resonances of the magma column.

Fitting the theory to the data, as was done for Fig. 5, is relatively straightforward because several of the features in the spectrum depend primarily on only one parameter and are insensitive to the others. For example, the minimum labeled E may be shifted to higher or lower frequencies in the theoretical spectrum by changing the depth of the source, leaving the positions of the longitudinal and radial resonances essentially unchanged. A similar separation occurs with the longitudinal resonance peaks, whose center frequencies are given by the expression

$$f_m = \frac{mc_2}{2L}, \quad m = 1, 2, \ldots . \tag{6.1}$$

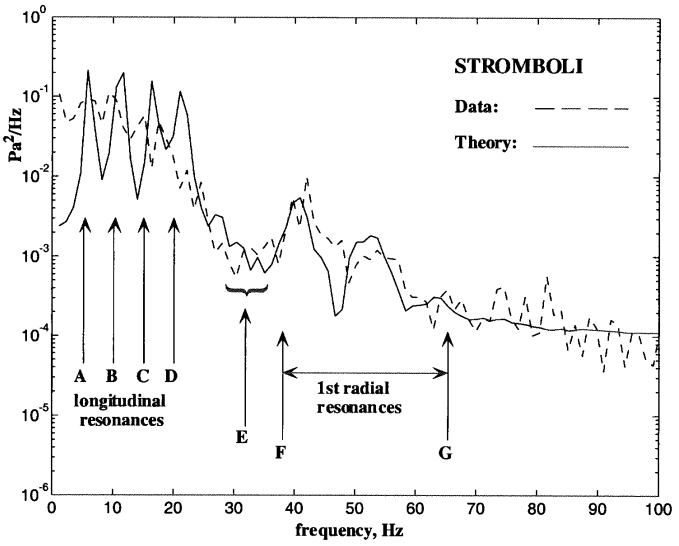

Fig. 5. Spectrum (measured and theoretical) of the airborne sound from an explosive event at Stromboli.

Clearly, these resonance frequencies will be shifted by altering the depth, L, of the magma column, but this leaves the position of the minimum at E and the radial resonances between F and G essentially unaffected.

Since each region of the spectrum is controlled primarily by a single geoacoustic parameter, the airborne acoustic spectrum provides the basis of a simple inversion technique. By fitting the theory to each region of the spectral data, as was done in Fig. 5, the depth and radius of the conduit, and the source depth, may all be estimated. Other features of the acoustic signature may also be useful in yielding additional information about the internal properties of the volcano. For instance, in the time domain, the duration of the pulse arrival may be inverted to obtain an estimate of the viscosity of the magma. Thus, the airborne sound may have potential as a remote sensing tool for determining not only the internal geometry of the volcano but also certain physical properties of the magma deep in the conduit.

7. Concluding Remarks

Although the theoretical model of a volcanic eruption as described above is geometrically rather simple, it leads to an airborne sound field of considerable complexity. The origin of the spatial and temporal structure in the acoustic field is the large number of normal modes, or resonances, that are supported by the magma column. It is interesting that the resonance characteristics of the sound field in the magma column are retained in the airborne acoustic field above the vent, even though the atmosphere itself is not a resonant cavity.

The detailed agreement between the theoretical and measured spectra of an explosive eruption at Stromboli volcano is striking, particularly in view of the simplified geometry

underpinning the theoretical model. This agreement occurs at low frequencies, below 60 Hz, where the wavelengths are long compared with the aperture of the vent. At higher frequencies, where the spectral structure of the airborne sound field is rich in complexity, our simple model would not be expected to match the observations with sensible accuracy. In this regime of shorter wavelengths, numerical modeling will probably be necessary to take account of irregularities in the terrain surrounding the vent, sound speed variations with depth in the magma column, and several other factors that have been neglected in our model.

According to our low-frequency model, certain significant features of the airborne sound spectrum are controlled essentially independently by different parameters. For instance, source depth determines the position of a broad minimum in the spectrum, and depth of the magma column establishes the positions of the longitudinal resonances. Although much still needs to be done, such behavior suggests that the airborne sound from an explosive eruption could provide a potentially useful, and relatively simple, inversion tool for obtaining quantitative estimates of the geometric, geophysical and geochemical properties of the volcano.

Acknowledgements

This work was supported by the Office of Naval Research under grant number N00014-93-1-0054.

References

1. F. A. Perret, "Volcanological observations," (Carnegie Institute of Washington Publication, Washington D.C., 1950), p. 162.
2. A. F. Richards, "Volcanic sounds: investigation and analysis," *J. Geophys. Res.* **68**, 919 (1963).
3. A. T. E. Yuan, S. R. McNutt, and D. H. Harlow, "Seismicity and eruptive activity at Fuego volcano, Guatemala: February 1975–January 1977," *Journal of Volcanology and Geothermal Research* **21**, 277 (1984).
4. S. R. McNutt, "Observations and analysis of B-type earthquakes, explosions, and volcanic tremor at Pavlof volcano Alaska," *Bull. Seis. Soc. Am.* **76**, 153 (1986).
5. H. Okada, Y. Nishimura, H. Miyamachi, H. Mori, and K. Ishihara, "Geophysical significance of the 1988–1989 explosive eruptions of M. Tokachi, Hokkaido, Japan," *Bull. Volcan. Soc. Japan* **35**, 175 (1990).
6. E. Gordeev, "Modelling of volcanic tremor as explosive point sources in a single-layered, elastic half-space," *J. Geophys. Res.* **98**, 19,678 (1993).
7. M. Ripepe, M. Rossi, and G. Saccorotti, "Image processing of explosive activity at Stromboli," *J. Volcan. Geotherm. Res.* **54**, 335 (1993).
8. S. Vergniolle and G. Brandeis, "Origin of the sound generated by Strombolian explosions," *Geophys. Res. Lett.* **21**(18), 1959 (1994).
9. K. Uhira and M. Takeo, "The source of explosive eruptions of Sakurajima volcano, Japan," *J. Geophys. Res.* **99**, 17,775 (1994).
10. M. J. Buckingham and M. A. Garcés, "Canonical model of volcano acoustics," *J. Geophys. Res.* **101**, 8129 (1996).

11. K. Yamaoka, J. Oikawa, and Y. Ida, "An isotropic source of volcanic tremor — observation with a dense seismic network at Izu-Oshima volcano, Japan," *J. Volcan. Geotherm. Res.* **47**, 329 (1991).
12. K. Ishihara, "Dynamical analysis of volcanic explosion," *J. Geodyn.* **3**, 327 (1985).
13. T. Sekine, T. Katsura, and S. Aramaki, "Water saturated phase relations of some andesites with application to the estimation of the initial temperature and water pressure at the time of eruption," *Geochimica et Cosmochimica Acta* **43**, 1367 (1979).
14. R. H. Cole, *Underwater Explosions* (Princeton University Press, Princeton, NJ, 1948), p. 437.
15. D. E. Weston, "Underwater explosions as acoustic sources," *Proc. Physical Soc., London* **B76**, 233 (1960).
16. J. B. Gaspin, J. A. Goertner, and I. M. Blatstein, "The determination of acoustic source levels for shallow underwater explosions," *J. Acoust. Soc. Am.* **66**, 1453 (1979).
17. N. R. Chapman, "Measurement of the waveform parameters of shallow explosive charges," *J. Acoust. Soc. Am.* **78**, 672 (1985).
18. A. V. Oppenheim and R. W. Schafer, *Digital Signal Processing* (Prentice-Hall, Englewood Cliffs, 1975), p. 585.
19. G. Giberti, C. Jaupart, and G. Sartoris, "Steady-state operation of Stromboli volcano, Italy: Constraints on the feeding system," *Bull. Volcan.* **54**, 535 (1992).